We are IntechOpen,
the world's leading publisher of
Open Access books
Built by scientists, for scientists

6,900
Open access books available

185,000
International authors and editors

200M
Downloads

154
Countries delivered to

Our authors are among the

TOP 1%
most cited scientists

12.2%
Contributors from top 500 universities

CLARIVATE ANALYTICS
BOOK CITATION INDEX
INDEXED

WEB OF SCIENCE™

Selection of our books indexed in the Book Citation Index
in Web of Science™ Core Collection (BKCI)

Interested in publishing with us?
Contact book.department@intechopen.com

Numbers displayed above are based on latest data collected.
For more information visit www.intechopen.com

Optical Communication with Weak Coherent Light Fields

Kim Fook Lee, Yong Meng Sua and
Harith B. Ahmad

1. Introduction

Entanglement and superposition are foundations for the emerging field of quantum communication and information processing. These two fundamental features of quantum mechanics have made quantum key distribution unconditionally secure (Scarani et al., 2009; Weedbrook et al., 2010) compared to communication based on classical key distribution. Currently, implementation of an optical quantum communication is mainly based on discrete and continuous quantum variables. They are usually generated through nonlinear interaction processes in $\chi^{(2)}$ (Kwiat et al., 1995) and $\chi^{(3)}$ (Lee et al., 2006,2009) media. Discrete-variable qubit based implementations using polarization (Liang et al., 2006, 2007; Chen et al. 2007, 2008; Sharping et al., 2006) and time-bin (Brendel et al., 1999; Tittel et al., 1998, 1999) entanglement have difficulty to obtain unconditional-ness, and also usually have low optical data-rate because of post-selection technique with low probability of success in a low efficient single photon detector at telecom-band (Liang et al., 2005, 2006, 2007). Continuous-variable implementations using quadrature entanglement (Yonezawa et al., 2004; Bowen et al., 2003; Silberhorn et al., 2002) and polarization squeezing (Korolkova et al., 2002) can have high efficiency and high optical data-rate because of available high speed and efficient homodyne detection. However, the quality of quadrature entanglement is very sensitive to loss, which is imperfect for implementing any entanglement based quantum protocols over long distance. Continuous-variable protocols that do not rely on entanglement, for instance, coherent-state based quantum communication (Yuen, 2004; Corndorf et al., 2003; Barbosa et al., 2003; Grosshans et al., 2002, 2003; Qi et al., 2007; Wilde Qi et al., 2008), are perfect for long distance optical communication. Several experimental approaches were taken to resolve transmission loss for long distance optical communication by using coherent light source. Optical wave

mechanical implementations (Lee et al., 2002, 2004) of entanglement and superposition with coherent fields have been demonstrated.

We discuss and demonstrate a new type of optical communications based on weak coherent light fields in detail in this chapter.

2. Correlation functions of two weak light fields

Two orthogonal light fields are used to implement correlation function between two distant observers. In the Stapp's approach (Grib et al., 1999; Peres, 1995) for two distant observers A and B, when analyzer A is oriented along the polarization angle θ_1, the transmitted $|\theta_1\rangle_{//}$ and reflected $|\theta_1\rangle_{\perp}$ polarization vectors of the light are given by,

$$|\theta_1\rangle_{//} = \cos\theta_1 |H_1\rangle + \sin\theta_1 |V_1\rangle, \tag{1}$$

$$|\theta_1\rangle_{\perp} = -\sin\theta_1 |H_1\rangle + \cos\theta_1 |V_1\rangle, \tag{2}$$

where the **H** and **V** are the horizontal and vertical axes. Analyzer **A** is a combination of half wave plate (HWP) and a polarization beam splitter (PBS) for projecting the linear polarization of the incoming photon. The operator associated with analyzer **A** can be represented by

$$\widehat{A}_1 = |\theta_1\rangle_{//}\langle\theta_1| - |\theta_1\rangle_{\perp}\langle\theta_1|, \tag{3}$$

$$\widehat{A}_1 = Cos2\theta_1 \left(|H_1\rangle\langle H_1| - |V_1\rangle\langle V_1|\right) + Sin2\theta_1 \left(|H_1\rangle\langle V_1| + |V_1\rangle\langle H_1|\right). \tag{4}$$

The operator A_1 has eigenvalues of ±1, such that,

$$\widehat{A}_1 |\theta_1\rangle_{//} = 1 |\theta_1\rangle_{//}, \tag{5}$$

$$\widehat{A}_1 |\theta_1\rangle_{\perp} = -1 |\theta_1\rangle_{\perp}. \tag{6}$$

Depending on the photon is transmitted or rejected by the analyzer. Similarly, the analyzer **B** oriented at θ_2 can be defined as operator B_2,

$$\widehat{B}_2 = Cos2\theta_2 \left(|H_2\rangle\langle H_2| - |V_2\rangle\langle V_2|\right) + Sin2\theta_2 \left(|H_2\rangle\langle V_2| + |V_2\rangle\langle H_2|\right). \tag{7}$$

Operator $A_1(B_2)$ with eigenvalues of ±1 can be measured by using the balanced detection scheme as shown in Fig. 1. Two detectors are placed at the two output ports of a cube polarization beam splitter. Their output currents are subtracted from each other. The arrangement of this detection scheme can be used for measuring operator A_1 of Eq.(4) and B_2 of Eq.(7) that is the subtraction between the projection of the transmitted signal $D_{//}$ and the projection of the reflected signal $D_\perp$.

Let's consider a beam of photons incidents on the PBS, if one photon goes through the PBS, it will produce non-zero signal at detector $D_{//}$ and zero signal at detector $D_\perp$. Then, the subtraction yields positive signal as of $D_{//} - D_\perp \geq 0$. If a photon is reflected from the PBS, it will go to the detector $D_\perp$ and produce non-zero signal at detector $D_\perp$ and zero signal at detector $D_{//}$. Then, the subtraction yields negative signal as of $D_{//} - D_\perp \leq 0$. For a certain amount of time, the subtraction records the random positive and negative spikes corresponding to the eigenvalues of +1 and -1 of operator A_1, respectively, as shown in the inset of Fig. 1.
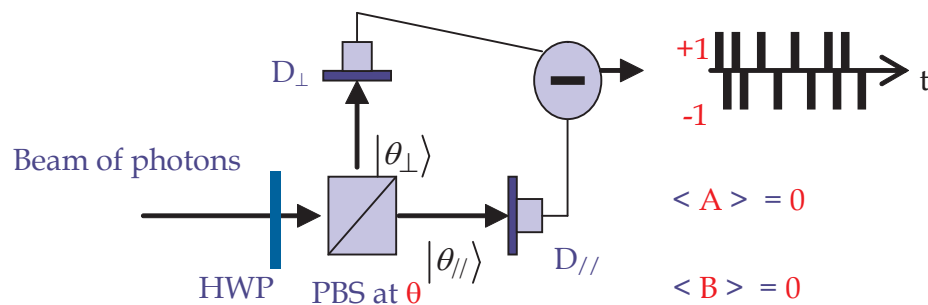

Figure 1. Detection scheme based on balanced homodyne detection for measuring operators A_1 and B_2.

If the incoming photons are in the superposition of $|\theta_1\rangle_{//}$ and $|\theta_1\rangle_\perp$, the detection scheme A records a series of discrete random values, +1 and -1. Then, the mean value of A_1 is zero, that is $\langle A_1 \rangle = 0$. Similarly, we can apply the same detection scheme for measuring operator B_2 and obtain $\langle B_2 \rangle = 0$. The expectation value of the product $\langle A_1 B_2 \rangle$ or the mean value of the product signals of A_1 and B_2 will produce correlation functions, as given by,

$$C(\theta_1, \theta_2) \propto \langle A_1 B_2 \rangle \propto \pm \cos 2(\theta_1 \pm \theta_2). \tag{8}$$

As shown in Eq.(8) above, there are 4 type of correlation functions analog to four Bell states. Theoritical prediction for the mean value measurements of $\langle A_1 B_2 \rangle$ are shown in Fig. 2.
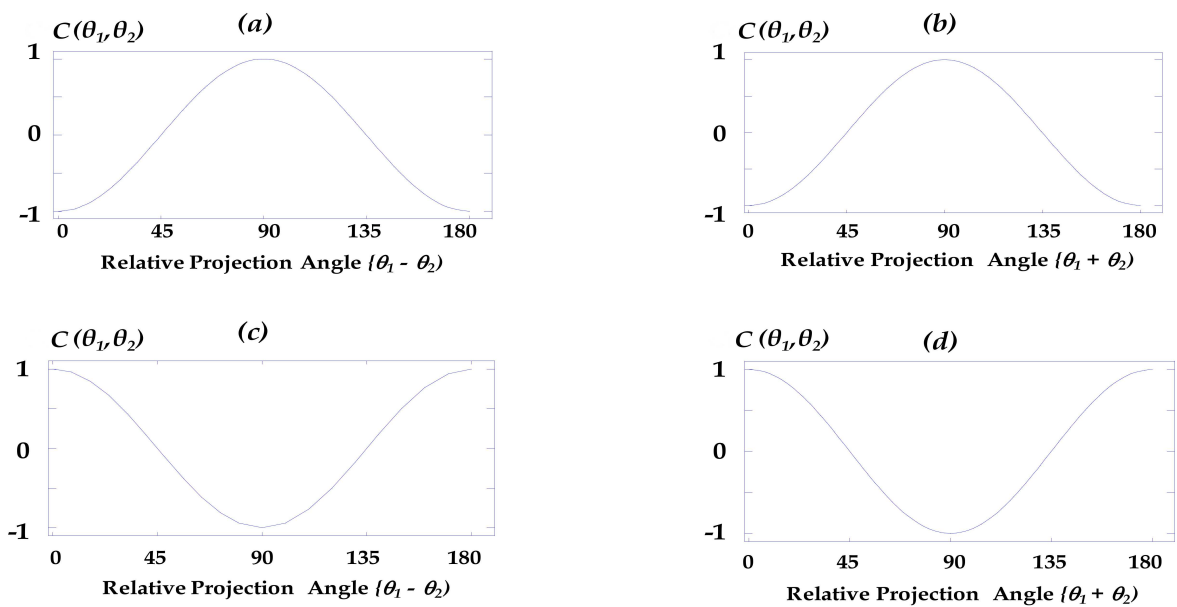
Figure 2. Theoritical prediction of correlation functions (a) $-\cos 2(\theta_1 - \theta_2)$, (b) $-\cos 2(\theta_1 + \theta_2)$, (c) $\cos 2(\theta_1 - \theta_2)$, (d) $\cos 2(\theta_1 + \theta_2)$.

3. Balanced homodyne detector

Balanced homodyne detector is utilised as the detection scheme for the weak coherent light fields for optical communication.

It consists of a 50/50 beam splitter, two photo detectors, a local oscillator field and a transimpendance amplifier. Superposed local oscillator field and weak light field will be detected by photodiodes D_1 and D_2, lead to the generation of the photocurrent I_1 and I_2. The photodiodes are connected together in such a way that the output equal to the I_1 minus I_2 as shown in Fig. 3.
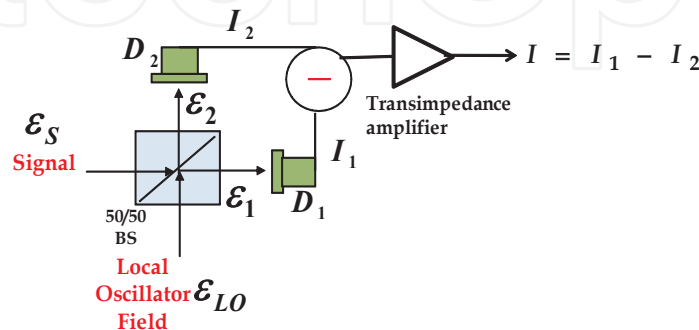

Figure 3. Balanced Homodyne detection.

The balanced detector has two input ports. The signal field and local oscillator field optically mixed at the beam splitter. The local oscillator field is a large amplitude lightwave with the same frequency as the signal and having a well-defined phase with respect to the signal field. Generally, local oscillator field can be obtained from the same laser source as the signal field. The emerging output fields ε_1 and ε_2 are the superposition of signal and local oscillator fields. The output fields ε_1 and ε_2 are given as,

$$\varepsilon_1 = \frac{1}{\sqrt{2}}(\varepsilon_{LO} + \varepsilon_s), \quad \text{(a)}$$

$$\varepsilon_2 = \frac{1}{\sqrt{2}}(\varepsilon_{LO} - \varepsilon_s). \quad \text{(b)} \tag{9}$$

where ε_{LO} and ε_s are the amplitude of the signal and local oscillator field respectively. Photocurrents that produced by the output fields ε_1 and ε_2 are given as

$$I_1 = |\varepsilon_1|^2 = \varepsilon_1 \varepsilon_1^*, \tag{10}$$

$$I_2 = |\varepsilon_2|^2 = \varepsilon_2 \varepsilon_2^*. \tag{11}$$

Hence, the output of the balanced homodyne detector will be given as,

$$I_1 - I_2 = 2\varepsilon_s \varepsilon_{LO}. \tag{12}$$

Since the signal and local oscillator fields are derived from the same laser source with relative phase φ. By considering only the real part of the signal and local oscillator fields, it can be described as,

$$\varepsilon_s = A\varepsilon_s Cos(\omega t), \tag{13}$$

$$\varepsilon_{LO} = A\varepsilon_{LO} Cos(\omega t + \varphi). \tag{14}$$

Where $A\varepsilon_s$ and $A\varepsilon_{LO}$ are the amplitude for signal and local oscillator fields, ω is optical frequency, φ is relative phase between the fields. Hence the output of the balanced homodyne detector is given by,

$$I_1 - I_2 = |A\varepsilon_s||A\varepsilon_{LO}|\{\cos(\varphi) + \cos(2\omega t + \varphi)\}. \tag{15}$$

The second term in the Eq.(15) is the fast varying term beyond the detection of the of the photo detector. Therefore, the output of the balanced homodyne detector is phase dependence, which is given by,

$$I_1 - I_2 \propto |A\varepsilon_s||A\varepsilon_{LO}|\cos(\varphi). \tag{16}$$

One of the main features of the balanced homodyne detector is the high signal to noise ratio compared to a single detector. For example, classical intensity fluctuations of the laser would affect the measurement of a single detector. Contrary, any changes in intensity will be canceled by the subtraction of the photocurrent with an ideal balanced homodyne detector.

However, due to the Poissonian statistics of the coherent light and random splitting process in the 50/50 beam splitter, fluctuations in intensity cannot be completely removed. Therefore even with the presence of only local oscillator field, the balanced homodyne detector will have a shot noise level above the electronics noise level as depicted in Fig.4, limiting the signal to noise ratio.
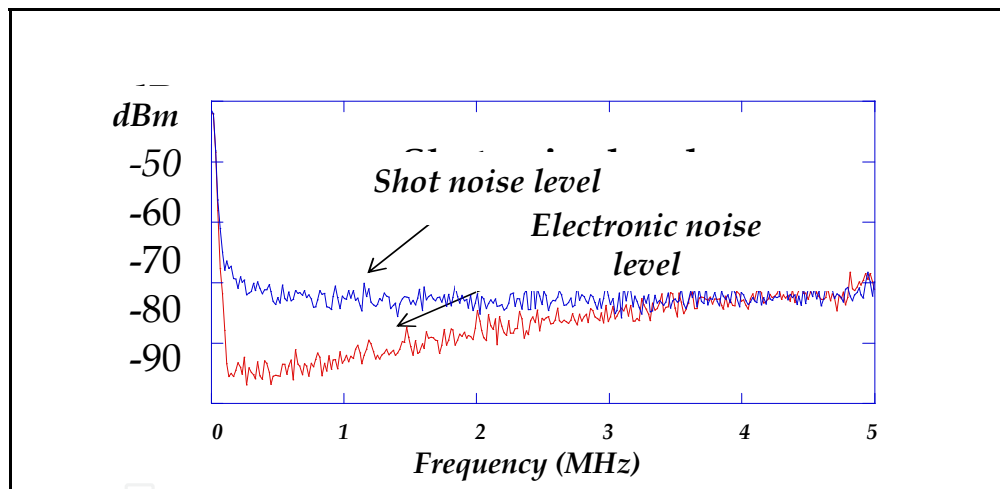

Figure 4. Frequency spectrum of balanced homodyne detector. The red line is the electronics noise of the BHD without any light while the blue line is the shot noise level of the BHD with the presence of the local oscillator field.

4. Practical demonstration of the optical communication with two weak light fields

A proof-of-principle experiment to demonstrate the correlations of two weak light fields as described in section 2 is shown in Fig.5. A continuous wave laser at telecom band wavelength (1534nm) is used to provide two orthogonal weak light fields. We use a 50/50 beam splitter to optically mix the vertically and horizontally polarized coherent light fields. The beam 1 from

the output port 1 of the beam splitter is a superposition of the vertically and horizontally polarized weak light fields, similarly for beam 2 from output port 2 of the beam splitter. The balanced homodyne detectors are made of two p-i-n photodiodes (EXT500) and the signal measured by the balanced homodyne detectors will be further amplified by a transimpedance amplifier. A quarter wave plate at 45° as part of measuring device is inserted at beams 1 and 2 to transform the linearly polarized states to circularly polarized states. By using a quarter wave plate transformation matrix, the field amplitudes V_1, H_1, V_2 and H_2 are transformed as,

$$
\begin{aligned}
V_1 &\to -i\hat{H}_1 + \hat{V}_1, &\text{(a)} \\
H_1 &\to \hat{H}_1 - i\hat{V}_1, &\text{(b)} \\
V_2 &\to -i\hat{H}_2 + \hat{V}_2, &\text{(c)} \\
H_2 &\to \hat{H}_2 - i\hat{V}_2, &\text{(d)}
\end{aligned}
\tag{17}
$$

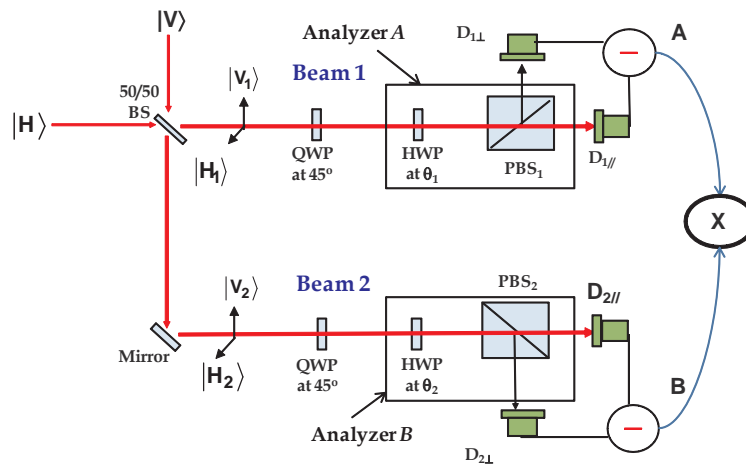where the phase shift due to the beam splitter is included.

Figure 5. Experimental setup for demonstration of the optical communication with weak coherent light fields.

For simplicity we use unit vector notation and drop the amplitude of field notation. Now, analyzer A in beam 1 will experience homogeneous superposition of left circularly polarized and right circularly polarized weak light fields. Similarly for analyzer B in beam 2. Analyzer $A(B)$ is placed before the balanced homodynes detector $A(B)$ to project out the phase angle 1(2) as,

$$
\hat{e}_1 \to \cos\theta_1 \hat{H}_1 + \sin\theta_1 \hat{V}_1,
\tag{18}
$$

$$
\hat{e}_2 \to \cos\theta_2 \hat{H}_2 + \sin\theta_2 \hat{V}_2.
\tag{19}
$$

The superposed field in beam 1 after the $\lambda/4$ wave plate and the analyzer can be expressed as,

$$
\begin{aligned}
E_1(t) &= [(\hat{H}_1 - i\hat{V}_1)e^{-i(wt+\varphi)}] + (i\hat{H}_1 - \hat{V}_1)e^{-iwt}] \cdot \hat{e}_1 \\
&= (-\cos\theta_1 + i\sin\theta_1)e^{-i(wt-i\varphi)} \\
&\quad + (-i\cos\theta_1 + \sin\theta_1)e^{-iwt}.
\end{aligned}
\tag{20}
$$

and similarly for the superposed field in beam 2,

$$
\begin{aligned}
E_2(t) &= [(\hat{H}_2 - i\hat{V}_2)e^{-i(wt+\varphi)}] + (i\hat{H}_2 - \hat{V}_2)e^{-iwt}] \cdot \hat{e}_2 \\
&= (-\cos\theta_2 + i\sin\theta_2)e^{-i(wt+\varphi)} \\
&\quad + (-i\cos\theta_2 + \sin\theta_2)e^{-iwt},
\end{aligned}
\tag{21}
$$

where ω is optical frequency, and φ is the relative phase of the two orthogonal weak light fields. Thus, the interference signals obtained by the photodetector $D_{1//}$ in balanced homodyne detectors at beam 1 are given as,

$$
\begin{aligned}
D_{1//}(\varphi) &= -ie^{-i(2\theta_1+\varphi)} + c.c \\
&\propto \sin(2\theta_1 + \varphi). &\text{(a)} \\
D_{1\perp}(\varphi) &= ie^{-i(2\theta_1+\pi+\varphi)} + c.c \\
&\propto -\sin(2\theta_1 + \varphi). &\text{(b)}
\end{aligned}
\tag{22}
$$

On the other hand, for photodetector $D_{2//}$, the reflected beat signal becomes 22b

Then, the balanced detector A measures

$$
\begin{aligned}
A_1(\varphi) &= D_{1//} - D_{1\perp} \\
&= 2\sin(2\theta_1 + \varphi).
\end{aligned}
\tag{23}
$$

Similarly, the interference signals obtained by the photodetectors in balanced homodyne detector at beam 2 can be written as,

$$
\begin{aligned}
D_{2//}(\varphi) &= ie^{-i(2\theta_2+\pi+\varphi)} + c.c \\
&\propto -\sin(2\theta_2 + \varphi), &\text{(a)} \\
D_{2\perp}(\varphi) &= -ie^{-i(2\theta_2+\pi+\varphi)} + c.c \\
&\propto \sin(2\theta_2 + \varphi), &\text{(b)}
\end{aligned}
\tag{24}
$$

and the balanced detector **B** measures

$$
\begin{aligned}
B_2(\varphi) &= D_{2//} - D_{2\perp} \\
&= -2\sin(2\theta_2 + \varphi).
\end{aligned}
\tag{25}
$$

The interference signals of Eq.(23) and Eq.(25) above for balanced detectors **A** and **B** are the measurements of operators A_1 and B_2, respectively. The interference signal in detector **A** is anti-correlated to detector **B** because of the phase shift of the beam splitter. The interference signals contain information of the projection angles of the analyzers. The average of the interference signals is zero, that is, $<A_1> = 0$ and $<B_2> = 0$. To further discuss the significant of measuring the operator A_1, the interference signals obtained in balanced detector **A** can be rewritten as,

$$
A_1(\varphi) = 2\{\cos(2\theta_1)\sin(\varphi) + \sin(2\theta_1)\cos(\varphi)\},
\tag{26}
$$

which is identical in structure with operator A_1 as in Eq.(4), that is

$$
\widehat{A}_1 = Cos2\theta_1\left(\left|H_1\right\rangle\left\langle H_1\right| - \left|V_1\right\rangle\left\langle V_1\right|\right) - Sin2\theta_1\left(\left|H_1\right\rangle\left\langle V_1\right| + \left|V_1\right\rangle\left\langle H_1\right|\right).
\tag{27}
$$

The factor of 2 in Eq.(26) is due to the 3 dB gain obtained by balanced detection scheme. Note that the unit polarization projectors $\left(\left|H_1\right\rangle\left\langle H_1\right| - \left|V_1\right\rangle\left\langle V_1\right|\right)$ and $\left(\left|H_1\right\rangle\left\langle V_1\right| + \left|V_1\right\rangle\left\langle H_1\right|\right)$ in Eq.(27) can be interpreted by in-phase and out-of-phase components of the light field. Similarly for the interference signals obtained in balanced detector B.

The interference signals in detectors **A** and **B** are then multiplied to obtain the anti-correlated multiplication signal,

$$
\begin{aligned}
A_1 \times B_2 &\propto -\sin(2\theta_1 + \varphi)\sin(2\theta_2 + \varphi) \\
&\propto -\cos(2(\theta_1 - \theta_2)) - \cos(2(\theta_1 + \theta_2 + \varphi)).
\end{aligned}
\tag{28}
$$

Then, the mean value of this multiplied signal is measured. We obtain one of the correlation functions $C(\theta_1, \theta_2)$ as described in section 2,

$$
\overline{A_1 \times B_2} \propto C(\theta_1, \theta_2) \propto -\cos 2(\theta_1 - \theta_2),
\tag{29}
$$

where the second term in Eq.(26) is averaging to zero due to the slow varying relative phase φ of the two orthogonal weak light fields from 0 to 2π. We normalized the correlation function $C(\theta_1, \theta_2)$ with its maximum obtainable value that is, $\theta_1 = \theta_2$. Thus, for the setting of the

analyzers at $\theta_1 = \theta_2$, the normalized correlation function $C(\theta_1, \theta_2) = -1$ shows that the two beams are anti-correlated. To generate other correlation functions, such as $C(\theta_1, \theta_2) \propto -\cos 2(\theta_1 + \theta_2)$ the $\lambda/4$ wave plate at beam 2 is rotated at -45°, then the beat signal measured by balanced homodyne detector B_2 of Eq.(25) is given by

$$B_2(\varphi) \propto D_{2//}(\varphi) - D_{2\perp}(\varphi) \propto -2\sin(2\theta_2 - \varphi). \tag{30}$$

Hence, obtaining the correlation function,

$$C(\theta_1, \theta_2) \propto -\cos 2(\theta_1 + \theta_2). \tag{31}$$

As for correlation function $C(\theta_1, \theta_2) \propto \cos 2(\theta_1 - \theta_2)$ a $\lambda/2$ plate in beam 2 is inserted, then the minus sign of beat signal B_2 of Eq.(30) is changed to positive sign, yielding the desired correlation function. Similarly, with the $\lambda/2$ wave plate at beam 2 and the $\lambda/4$ wave plate at beam 2 rotated at -45°, the beat signal B_2 of Eq.(30) is equal to $2\sin(2\theta_2 - \varphi)$. Thus, providing the last correlation function $C(\theta_1, \theta_2) \propto \cos 2(\theta_1 + \theta_2)$.

4.1. Correlation measurement of a stable field and a noise field

To verify the above analysis and measurement method for weak light fields, we present an experiment measurement of one stable coherent light field and one random noise phase modulated light field.

One stable coherent field is mixed with one noise field in a beam splitter. The experimental result has been recently published(Lee, 2009). Fig. 6(a) and (b) are the beat signals obtained at A and B, where the phase $\phi_c(t)$ is modulated with random noise through an acousto-optic modulator. The product of the beat signal at A and B is shown in Fig. 6(c). The mean-value measurement produces the bipartite correlation $-cos2(\theta_1 - \theta_2)$, which is still classical correlation. However, it is obvious that the information of θ_1 and θ_2 are protected by classical noise not quantum noise. Classical noise is not completely random compared to quantum noise as inherited by coherent state.

In the next section, two weak coherent light fields $|\alpha\rangle$ and $|\beta\rangle$ are used for generating quantum correlation, where the quantum noise $\phi(t) = \phi_\beta - \phi_\alpha$ provided by mean photon number fluctuation.

4.2. Correlation measurement of two weak light fields

By using the experiment setup as proposed in Fig.5, we are able to generate 4 types of bipartite correlation, given as

$$C(\theta_1, \theta_2) \propto \pm\cos 2(\theta_1 \pm \theta_2). \tag{32}$$
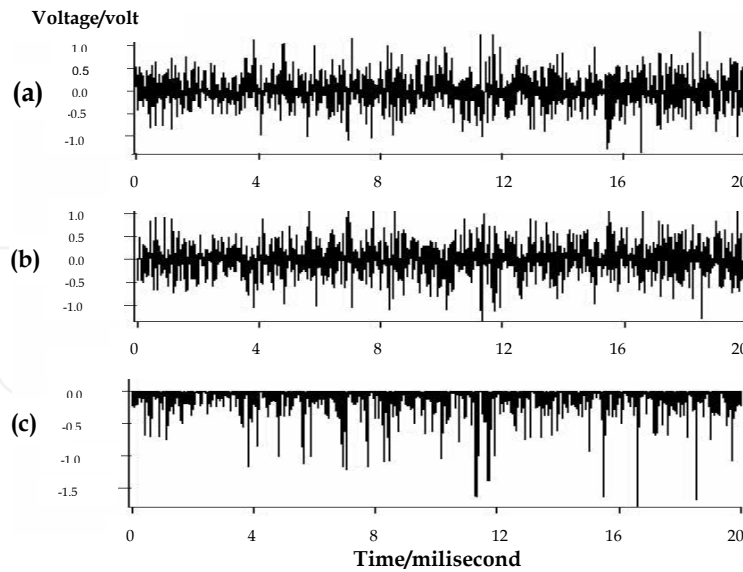
Figure 6. (a) The beat signal at balanced detector **A** (b) the beat signal at balanced detector **B** (c) the multiplied beat signal.

To verify the analysis discussed in section 2, we perform systematic studies of the proposed experiment. We use a piezoelectric transducer (PZT) to modulate the phase of a weak light field. Then, all 4 types of correlation function were obtained by manipulation of experiment setup as discussed in previous section. We normalized the correlation function *-cos 2(θ_1-θ_2)* with its maximum obtainable value, that is θ_1=θ_2. Fig.7 shows the normalized correlation function *±cos 2(θ_1 ± θ_2)* as a function of the relative projection angle of the analyzer *A* and *B*. The blue line is the predicted theoretical value while the red circle with the error bar is the experimental data.

For each data point, we take ten measurements of the multiplied signal and obtain the average mean value. Each measurement was obtained by fix the projection angle of the analyzer A and rotates the projection angle of analyzer B. The error bar is mainly due to the electronic noises and temperature dependence of polarization optics.

4.3. Bit generation and measurement

After we established one of the bipartite correlation functions between observer A and B, bit generation and measurement for optical communications can be done by implementing bit correlations between them.

Lock-in-amplifier is used to measure the bit correlation of between observer *A* and *B*. Fig.8 depicts the experimental setup for bit measurement for observer *A* and *B*. To perform this measurement for the established correlation function of *–cos 2(θ_1 − θ_2)*, we ramp the Piezo-electric transducer (PZT) at one of the weak light field to obtain one period of interference signal. An example of single period of interference signal measured at observer and reference signal for the lock-in amplifier is shown in Fig.9. For practical optical communication, phase locking of the two orthogonal weak light fields are required.
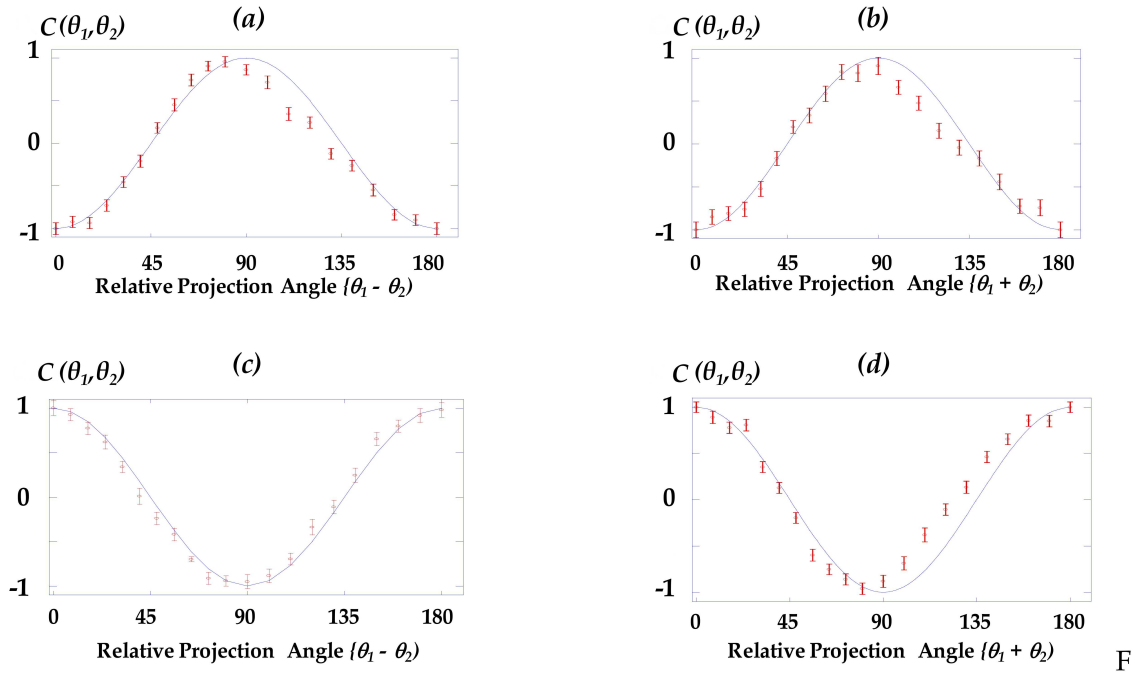
Figure 7. Experimental measurement of Bi-partite correlation functions (a)*–cos 2(θ₁ – θ₂)*, (b) *–cos 2(θ₁ + θ₂)*, (c) *cos 2(θ₁ – θ₂)*, (d) *cos 2(θ₁ + θ₂)*
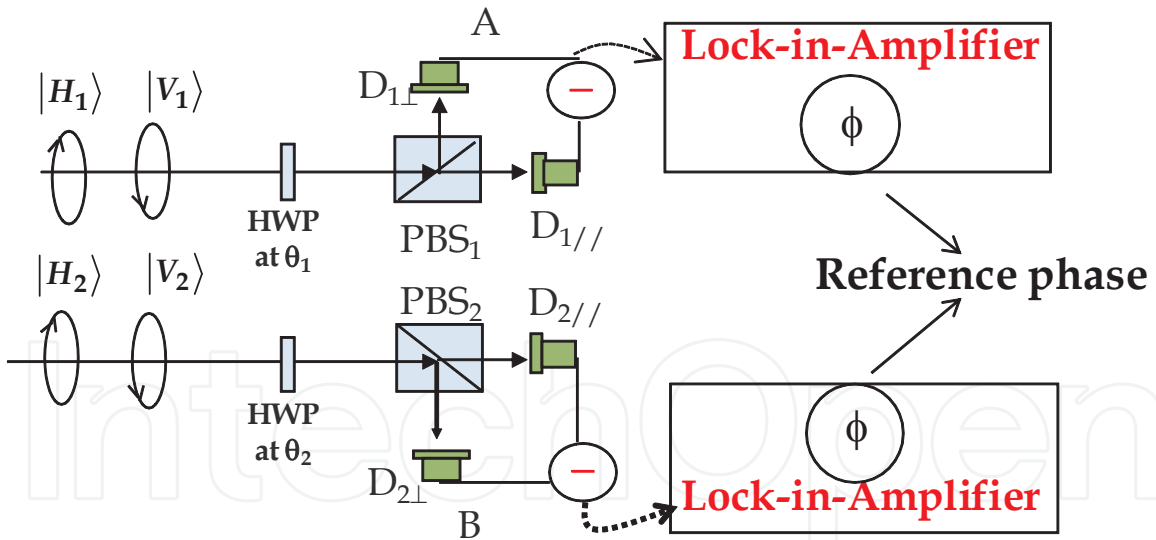

Figure 8. Experimental setup for demonstration of the bit generation and measurement

We measure quadrature phases of orthogonal weak light fields with the step size of $n\pi/2$ (n = integer) as shown in Fig. 10(a) (blue line). Using the same lock-in reference phase in the lock-in amplifier, we measure the quadrature phases of weak coherent state at detector **B** as shown in Fig. 10(a) (dashed red line). We have observed the bits correlation between two parties for the shared correlation function of $-cos\ 2(\theta_1 - \theta_2)$ as shown in Fig. 4(a), where the positive
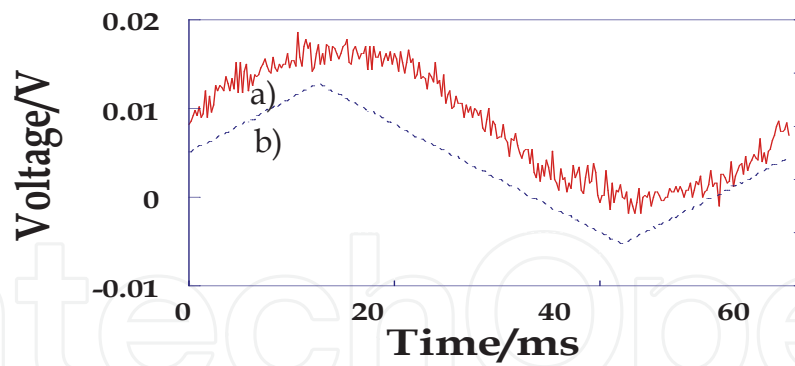
Figure 9. (a) Single period of interference signal measured at observer **A** (red line) compared to b) piezoelectric driving voltage (blue dashed line), which is used as reference phase in the lock-in amplifier.
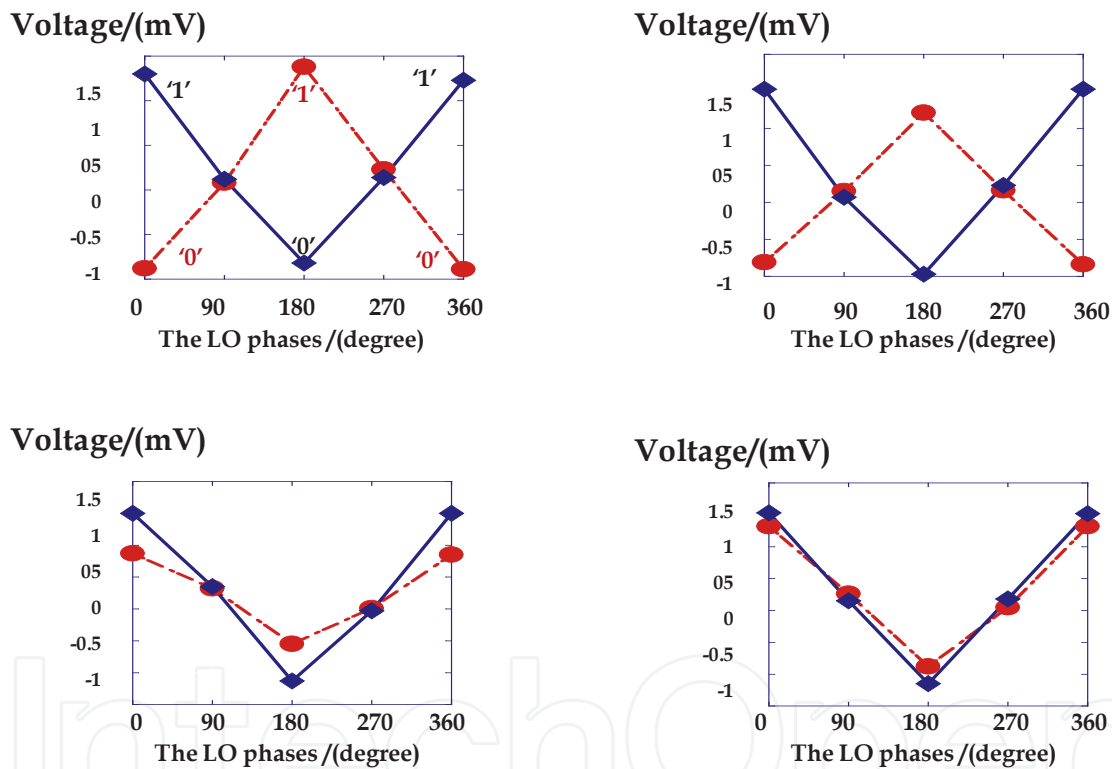

Figure 10. Bit correlation of two weak light fields (a) **–cos 2(θ₁ – θ₂)**, (b) **–cos 2(θ₁ + θ₂)**, (c) **cos 2(θ₁ + θ₂)**, and (d) **cos 2(θ₁ – θ₂)**

(negative) quadrature signal is encoded as keys/bits '1' ('0'), respectively. By using the same lock-in reference phase, we observe bits correlations for the other three types of correlation functions $-cos\ 2(\theta_1 + \theta_2)$, $cos\ 2(\theta_1 + \theta_2)$, and $cos\ 2(\theta_1 - \theta_2)$ as shown in Figs. 10(b), 10(c), and 10(d), respectively.

In real practice of long distance optical communication, we can establish one of the bit correlations for calibrating the lock-in reference phase at observer **A** and **B**. We further explore the feasibility of the scheme long distance optical communication for by performing bits

correlations between two observers over a distance of 10 km through a transmission fiber. We couple one of the orthogonal weak light fields into 10 km of transmission fiber and a quarter-wave plate and a half-wave plate are used at the output of the transmission fiber to compensate the birefringence. The correlation between two observers *A* and *B* are found to be preserved over the 10 km transmission fiber (Sua et al., 2011). We managed to establish four types of correlation functions and performed bits correlations for each shared correlation function between two observers.

In short, for our proposed weak coherent light fields optical communication scheme, information is encoded onto the superposition of the vertically and horizontally polarized weak light fields; decoding involves detection of the weak light fields by balanced homodyne detector and quadrature phases measurement by lock-in amplifier. For reliable measurement of the encoded signal, both phase and polarization of the weak light field must be stable.

Apparently, stability and accurate control of phase and polarization turned out to be the main challenge for the practical implementation of weak coherent light fields optical communication. The state of polarization of the light wave is not preserved in the typical transmission fiber. Dynamic control of the state of polarization of the light is critical to ensure the reliability the proposed optical communication scheme. Each dynamic polarization controller is bulky and expensive (Noe et al., 1999), severely limits the practicality of our scheme. Phase locking is another challenging obstacle as well. Phase locking is required between the two orthogonal weak light fields that used to implement the bit correlation between two observers. Without the phase locking, quadrature phases measurement performed by lock-in amplifier is meaningless. Therefore, optical phase-locked loop must be employed for the phase locking of two weak light fields. However, for high data rate optical communication, the delays allowed in the phased-locked loop are so small that phase locking becomes an enormous challenge (Barry et al., 1992; Kazovsky, 1986).

5. Conclusion

We have experimentally demonstrated a new type of optical communication protocol based on weak coherent light fields. Coherent bipartite quantum correlations of two distant observers are generated and used to implement keys (bits) correlation over a distance of 10 km. Our scheme can be used to provide security as a supplement to the existence decoy-state Bennett-Brassard 1984 protocol and the differential phase-shift quantum key distribution (DPS-QKD) protocol. The realization of intrinsic correlation of weak coherent light fields by using the measurement method is a first step toward linear-optics quantum computing with weak light fields and single-photon source.

Acknowledgements

Author details

Kim Fook Lee[1], Yong Meng Sua[1] and Harith B. Ahmad[2]

1 Department of Physics, Michigan Technological University, Houghton, Michigan, USA

2 Department of Physics, University of Malaya, Kuala Lumpur, Malaysia

References

[1] Barbosa, G. A.; Corndorf, E.; Kumar, P. & Yuen, H. P. (2003). Secure Communication using Mesoscopic coherent states, Phys. Rev. Lett., Vol.90, pp227901

[2] Barry, J. R. & Kahn, J. M. (1992). Carrier synchronization for homodyne and heterodyne-detection of optical quadriphase-shift keying, J. Lightwave Technol., Vol.10, pp1939–1951

[3] Bhattacharya, N.; van Linden van den Heuvell, H. B. & Spreeuw, R. J. C. (2002). Implementation of Quantum Search Algorithm using Classical Fourier Optics, Phys. Rev. Lett., Vol. 88, pp137901

[4] Bigourd, D.; Chatel, B.; Schleich, W. P. & Girard, B. (2008). Factorization of Numbers with the Temporal Talbot Effect: Optical Implementation by a Sequence of Shaped Ultrashort Pulses, Phys. Rev. Lett., Vol.100, pp030202

[5] Bowen, W. P.; Schnabel, R.; Lam, P. K.; & Ralph, T. C. (2003). Experimental Investigation of Criteria for Continuous variable entanglement, Phys. Rev. Lett., Vol.90, pp043601

[6] Brendel, J.; Gisin, N.; Tittel, W. & Zbinden, H. (1999). Pulsed energy-time entangled twin-photon source for quantum communication. Phys. Rev. Lett., Vol.82, pp2594

[7] Chen, J.; Lee, K. F.; and Kumar, P. (2007). Deterministic quantum splitter based on time-reversed Hong-Ou-Mandel interference, Phys. Rev. A, Vol.76, pp031804(R)

[8] Chen, J.; Altepeter, J. B.; Medic, M.; Lee, K. F.; Gokden, B.; Hadfield, R. H.; Nam, S. W. & Kumar, P. (2008). Demonstration of a Quantum Controlled-NOT Gate in the Telecommunications Band, Phys. Rev. Lett., Vol.100, pp133603

[9] Corndorf, E.; Barbosa, G. A.; Liang, C.; Yuen, H. P. & Kumar, P. (2003). High-speed data encryption over 25 km of fiber by two-mode coherent state quantum cryptography, Opt. Letters. Vol.28, pp2040-2042

[10] Grib, A.A.; & Rodrigues, W. A. (1999). Nonlocality in Quantum Physics, Springer, ISBN 030646182X, New York, USA

[11] Grosshans, F. & Grangier, P. (2002). Continuous variable quantum cryptography using coherent states, Phys. Rev. Lett., Vol.88, pp057902

[12] Grosshans, F.; Assche, G. V.; Wenger, J.; Brouri, R.; Cerf, N. J.; & Grangier, P. (2003). Quantum key distribution using gaussian-modulated coherent states, Nature, Vol.421, pp238

[13] Kazovsky, L. (1986). Balanced phase-locked loops for optical homodyne receivers: performance analysis, design considerations, and laser linewidth requirements, J. Lightwave Technol. ,Vol.4, pp182–195

[14] Korolkova, N.; Leuchs, G.; Loudon, R.; Ralph, T.; & Silberhorn, C. (2002). Polarization squeezing and continuous-variable polarization entanglement, Phys. Rev. A, Vol.65, pp052306

[15] Kwiat, P. G; Mattle, K.; Weinfurter, H.; Zeilinger, A.; Sergienko, A. V. & Shih, Y. (1995). New High-Intensity Source of Polarization-Entangled Photon Pairs, Phys. Rev. Lett., Vol.75, pp4337-4341

[16] Lee, K. F. & Thomas, J. E. (2002). Experimental Simulation of Two-Particle Quantum Entanglement using Classical Fields, Phys. Rev. Lett., Vol, 88, pp097902

[17] Lee, K. F.; Chen, J.; Liang, C.; Li,X.; Voss, P. L. & Kumar, P. (2006). Observation of high purity entangled photon pairs in telecom band, Optics Letters. Vol.31, pp1905

[18] Lee, K. F.; Kumar, P.; Sharping, J. E.; Foster, M. A.; Gaeta A. L.; Turner A. C.; & Lipson, M. (2008). Telecom-band entanglement generation for chipscale quantum processing, arXiv:0801.2606 (quant-ph)

[19] Lee, K. F. & Thomas, J. E. Entanglement with classical fields, (2004). Phys. Rev. A, Vol. 69, pp052311

[20] Lee, K. F. (2009). Observation of bipartite correlations using coherent light for optical communication, Optics Letters, Vol.34, pp1099-1101

[21] Liang, C.; Lee, K. F.; Voss, P. L.; Corndorf, E.; Gregory S.; Chen, J.; Li,X & Kumar, P. (2005). Single-Photon Detector for High-Speed Quantum Communication Applications in the Fiber-optic Telecom Band, Free-Space Laser Communications V. Edited by Voelz, David G. Ricklin, Jennifer C. Proceedings of the SPIE, Vol.5893, pp282-287

[22] Liang, C.; Lee, K. F.; Chen, J. & Kumar, P. (2006). Distribution of fiber-generated polarization entangled photon-pairs over 100 km of standard fiber in OC-192 WDM environment, postdeadline paper, Optical Fiber Communications Conference and the 2006 National Fiber Optic Engineers Conference, Anaheim Convention Center, Anaheim, CA

[23] Liang, C.; Lee, K. F.; Medic, M.; Kumar, P. & Nam, S. W. (2007). Characterization of fiber-generated entangled photon pairs with superconducting single-photon detectors, Optics Express, Vol.15, pp1322

[24] Noe, R.; Sandel, D.; Yoshida-Dierolf, M.; Hinz, S.; Mirvoda, V.; Schopflin, A.; Glingener, C.; Gottwald, E.; Scheerer, C.; Fischer, G.; Weyrauch, T. & Haase, W. (1999). Polarization mode dispersion compensation at 10, 20, and 40Gb/s with various optical equalizers, J. Lightwave Technol., Vol.17, pp1602–1616

[25] Peres, A. (1995). Quantum Theory: Concepts and Methods (Fundamental Theories of Physics), Springer, ISBN 0792336321, New York, USA

[26] Qi, B.; Huang, L. L.; Qian, L. & Lo, H. K. (2007). Experimental study on the Gaussian-modulated coherent state quantum key distribution over standard telecommunication fibers, Phys. Rev. A. Vol.76, pp052323

[27] Scarani, V.; Bechmann-Pasquinucci, H.; Cerf, N. J.; Dusek, M.; Lütkenhaus, N.; & Peev, M. (2009). Rev. Mod. Phys. Vol.81, pp1301

[28] Sharping, J. E.; Lee, K. F.; Foster, M. A.; Turner, A. C.; Lipson, M.; Gaeta, A. L.; & Kumar, P. (2006). Generation of correlated photons through parametric scattering in nanoscale silicon waveguides, Optics Express, Vol.14, pp12388,

[29] Silberhorn, C.; Ralph, T. C.; Lutkenhaus, N. & Leuchs, G. (2002). Continuous variable quantum cryptography: Beating the 3 dB loss limit, Phys. Rev. Lett., Vol.89, pp167901

[30] Sua, Y. M.; Scanlon, E.; Beaulieu, T.; Bollen, V. & Lee, K. F. (2011). Intrinsic quantum correlations of weak coherent states for quantum communication, Phys. Rev. A, Vol. 83, pp030302(R)

[31] Tittel, W.; Brendel, J.; Gisin, B.; Herzog, T.; Zbinden, H & Gisin, N. (1998). Experimental demonstration of quantum correlations over more than 10 km, Phys. Rev. A. Vol.57, pp3229.

[32] Tittel, W.; Brendel, J.; Zbinden, H & Gisin, N. (1999). Long distance Bell-type tests using energy-time entangled photons, Phys. Rev. A, Vol.59, pp4150.

[33] Weedbrook, C.; Lance, A.M.; Bowen, W.P.; Symul, T.; Ralph, T.C.; & Lam, P.K. (2004). Phys. Rev. Lett., Vol.93, pp170504.

[34] Wilde, M. W.; Brun, T. A.; Dowling, J. P.; & Lee, H. (2008). Coherent communication with linear optics, Phys. Rev. A, Vol.77, pp022321

[35] Yonezawa, H.; Aoki, T. & Furusawa, A. (2004). Demonstration of a quantum teleportation network for continuous variables, Nature, Vol.431, pp 430-433

[36] Yuen, H. P. (2004). KCQ: A New Approach to quantum cryptography I. General Principles and Key generation, quant-ph/0311061 v6